Published in final edited form as:
Curr Alzheimer Res. 2014 February ; 11(2): 128–136.

Identification of Human ABAD Inhibitors for Rescuing Aβ-Mediated Mitochondrial Dysfunction

Koteswara Rao Valasani[#], **Qinru Sun**[#], **Gang Hu**, **Jianping Li**, **Fang Du**, **Yaopeng Guo**, **Emily A Carlson**, **Xueqi Gan**, and **Shirley ShiDu Yan**[*]
Department of Pharmacology & Toxicology and Higuchi Bioscience Center, School of Pharmacy, University of Kansas, Lawrence, KS 66047 (USA)

Abstract

Amyloid beta (Aβ) binding alcohol dehydrogenase (ABAD) is a cellular cofactor for promoting (Aβ)-mediated mitochondrial and neuronal dysfunction, and cognitive decline in transgenic Alzheimer's disease (AD) mouse models. Targeting mitochondrial ABAD may represent a novel therapeutic strategy against AD. Here, we report the biological activity of small molecule ABAD inhibitors. Using *in vitro* surface plasmon resonance (SPR) studies, we synthesized compounds with strong binding affinities for ABAD. Further, these ABAD inhibitors (ABAD-4a and 4b) reduced ABAD enzyme activity and administration of phosphonate derivatives of ABAD inhibitors antagonized calcium-mediated mitochondrial swelling. Importantly, these compounds also abolished Aβ-induced mitochondrial dysfunction as shown by increased cytochrome c oxidase and adenosine-5′-triphosphate levels, suggesting protective mitochondrial function effects of these synthesized compounds. Thus, these compounds are potential candidates for further pharmacologic development to target ABAD to improve mitochondrial function.

Keywords

ABAD inhibitors; adenosine-5′-triphosphate; amyloid beta; benzothiazole amino phosphonates; cytochrome c oxidase; mitochondrial dysfunction

Introduction

Alzheimer's disease (AD) is a type of dementia in adults, which results in disordered cognition and memory due to neuronal stress and subsequent cell death. Multiple reports show that mitochondrial and synaptic dysfunction are early pathological features of AD [1-6]. In AD, amyloid beta (Aβ) progressively accumulates in synaptic mitochondria resulting in impaired mitochondrial structure and function [7-16]. Interaction of Aβ with mitochondrial proteins such as cyclophilin D, a key component of mitochondrial permeability transition pore, and Aβ-binding alcohol dehydrogenase (ABAD), a mitochondrial enzyme, enhances mitochondrial oxidative stress, mitochondrial toxicity and

[*]Correspondence should be addressed to Dr. Shirley ShiDu Yan, 2099 Constant Avenue, University of Kansas, Lawrence, KS 66047. shidu@ku.edu.
[#]Authors contributed equally to this work

Conflict of Interest: The authors confirm that this article content has no conflict of interest.

cognitive decline [3; 7; 9; 17-24]. Thus, strategies that suppresses or attenuates Aβ-induced mitochondrial toxicity in addition to decreasing Aβ levels in the brain may hold potential for preventing and/or halting AD at its early stages by improving mitochondrial function.

Hence, development of substances that inhibit Aβ function may result in more effective interventions for prevention and treatment interventions of AD. Scientists are exploring a number of strategies to block Aβ including “secretase inhibitors” to block the secretase clipping action [25-32]. It is not yet clear that any of these compounds will improve AD symptoms or protect neuronal cells, and none have entered clinical trials due to continuing concerns about side effects. Because AD is a multifaceted disease and its molecular biology is poorly understood, multi-targeted approaches will likely yield more effective treatments. As mitochondrial dysfunction is an early pathological feature of AD, targeting mitochondrial function could be an effective therapeutic strategy.

ABAD, unique among members of the short-chain dehydrogenase reductase family as it interacts with Aβ, has attracted considerable interest in AD drug discovery [9; 12; 33-36]. Increased ABAD expression was found in AD-affected brain regions (i.e., temporal gyrus and hippocampus) but not in AD-spared regions (i.e., cerebellum) as compared to age-matched, non-AD brain tissue [9; 37]. Similarly, transgenic (Tg) mice overexpressing amyloid precursor protein (APP)/Aβ showed higher ABAD levels in AD-affected hippocampus and cerebral cortex than nontransgenic littermate controls. Increased ABAD expression results in exaggerated mitochondrial oxidative stress, abnormal energy metabolism, and mitochondrial dysfunction in an AD mouse model [9; 12; 20; 38; 39]. Aβ interaction with ABAD inhibits normal enzymatic activity of ABAD, thereby promoting oxidative stress [9; 20], increasing mitochondrial toxicity [20], and inducing a signaling cascade that leads to apoptosis and accelerates early deficits in learning and memory [9]. Interestingly, our recent studies indicate that inhibition of ABAD-Aβ interaction protects mitochondria and neurons from Aβ-induced toxicity.

Recently, the search for inhibitors of ABAD-Aβ interactions has begun in the AD research field. Using an ELISA-based screening assay, an FDA-approved immunosuppressant drug called frentizole was identified as a novel inhibitor of ABAD-Aβ interactions. Analysis of the frentizole structure-activity relationship (SAR) studies allowed Xie et al. to develop new benzothiazole ureas with a 30-fold improvement in potency [33]. Previously, we designed and synthesized eight ABAD inhibitors based on the frentizole and benzothiazole ureas SAR studies; these inhibitors showed high affinity for binding to the human ABAD active site [40]. In the present study, we first evaluated the ABAD inhibitor activity of these novel benzothiazole phosphonate derivatives using *in vitro* surface plasmon resonance (SPR) to determine whether the synthetic compounds bind to human recombinant ABAD protein. Second, we examined the biological activity of these synthesized compounds on Aβ-induced mitochondrial function. Based on our SPR binding studies and biological activity, we selected these two compounds (i.e. 4a and 4b) for the present studies to characterize these novel potent drugs for prevention and treatment of AD by improving mitochondrial and neuronal function.

Materials and methods

Synthesis of ABAD inhibitors

We first synthesized the benzothiazole amino phosphonate derivatives using a three-component reaction of equimolar quantities of aromatic aldehydes, 6-methoxybenzo[d]thiazol-2-amine, and dimethyl phosphate in toluene at reflux temperature in the presence of Mg $(ClO_4)_2$ [40]. In this study, we used the two best compounds that had better biological activity based on binding affinity and effect on mitochondrial function induced by calcium or Aβ from our recently published paper [40]. Compounds ABAD-4a and 4b were in the form of white powder with melting points of 216°C and 180°C, and molecular weights of 452 and 394, respectively. The Molecular formulae for compound 4a is $C_{19}H_{22}N_2O_7PS$ and for 4b is $C_{17}H_{19}N_2O_5PS$ (Figure 1). High pressure liquid chromatography (HPLC) purity of the compounds 4a and 4b was 98% and 100%, respectively.

ABAD expression and purification

ABAD was produced recombinantly in *Escherichia coli* (BL21) and purified to homogeneity as previously described [41]. Briefly, BL21 *E. coli* were transformed with pGE5-human ABAD, prepared as described below. Transformants were induced with 0.5 mmisopropyl-1-thio-β-d-galactopyranoside for 3 h, and cell extracts were prepared by cell disruption. Extracts were subjected to cation exchange fast protein liquid chromatography (FPLC) chromatography on SP Sepharose Fast Flow (Amersham Pharmacia Biotech) and on Source 15S, followed by gel filtration on Superdex 200. The extract from 1 liter of bacterial culture was applied to 2 ml of SP Sepharose in 25 mM MES (pH 6.0), 50 mM NaCl, 5 mM dithiothreitol. The resin was washed with equilibration buffer and eluted with an ascending linear salt gradient (0.1–1.0 M NaCl).These fractions were pooled, diluted 6-fold, and applied to Source 15S resin in 0.1 M MES (pH 6.0)/0.1 M NaCl (5 mg of protein per 1 ml of resin). The column was eluted with an ascending salt gradient, and ABAD emerged at ≈0.15 M NaCl. ABAD-rich fractions were concentrated by ultrafiltration to ≈15 mg/ml and loaded onto a Superdex 200 (30/10) column (1 ml was applied to the column for each run). Peak fractions from Superdex 200 were subjected to immunoblotting for ABAD using specific antibody to ABAD generated in our Lab and used in our previous study The ABAD immunoreactive band was visualized at ≈27 kDa.

Binding Experiment with ABAD

We studied interactions between ABAD and compounds 4a and 4b using a dual flow cell as described previously [7; 9]. SPR studies were performed on a BIACORE 3000 at 25°C. SPR binding experiments with ABAD were performed in phosphate-buffered saline (PBS, pH 7.4, 0.005% surfactant P20), which served as both running and sample buffer. The surface of the sensor chip was first activated with mixtures of N-hydroxysuccinimide (NHS, 115 mg/ml) and N-(3-dimethyl-aminopropyl)-N′-ethyl-carbodiimide-hydrochloride (EDC, 750 mg/ml) for 7 minutes. ABAD was dissolved in PBS buffer (pH 5.0) at a concentration of 10 μg/ml. The protein was immobilized directly and covalently on the hydrophilic carboxy methylated dextran matrix of the CM5 sensor chip (Biacore) using the standard primary

amine coupling reaction according to standard procedures. After protein immobilization, excess activated carboxylic acid groups were quenched with ethanolamine (1 M, pH 8.5).

Care was taken during injection of samples to avoid carryover effects. Special washing routines were used to clean the system before injection of new samples. Sample flow rate was set at 40 μL/minute for the determination of the kinetic and equilibrium constant. Regeneration of the surfaces between subsequent binding experiments was achieved by washing the surface extensively with buffer solution.

All data analyses were carried out using BIA evaluation software, and sensor grams were processed by automatic correction for nonspecific bulk refractive index effects. Kinetic analyses of the ligand binding to the protein were performed based on the 1:1 Langmuir binding fit model according to the standard procedures described in the software manual.

Assay of ABAD enzymatic activity

ABAD activity was determined by inhibition of reduction of S-acetoacetyl-CoA (SAAC). The assay was carried out with human recombinant ABAD protein (418 ng/ml), SAAC (172 μM), NADH (102 μM), and a range of inhibitor concentrations (from 0 to 1000 μM) in 93 mM potassium phosphate buffer (pH 7.3) [41]. All assay components except SAAC were pre-incubated for 5 min; the reaction was initiated with the addition of SAAC. The reaction proceeded for 6 min at room temperature under steady-state conditions; the decrease NADH absorbance at 340 nm was determined every 10 seconds. Kinetic data was analyzed using PRISM software (Scitech, San Diego, CA) to determine IC_{50} value and Ki. One unit of enzyme activity was defined as the amount needed to convert 1.0 μmol of substrate to product per min.

Isolation of brain mitochondria

Brain cortex from mice without white matter was used for mitochondrial isolation. Mitochondria were prepared as previously described [7; 42]. Briefly, brain cortical tissues were homogenized in 9 ml of ice-cold EB buffer (EDTA 1 mmol, bovine serum albumin 1-6 mg/ml) using Dounce homogenizer until particles were no longer seen. Homogenates were centrifuged at 1300 × *g* for 5 min. Supernatant from this fraction was carefully deposited on top of 15% percoll solution (10 ml) and then centrifuged at 16000 RPM for 10 min. The pellet was carefully mixed with 9 ml of mitochondrial buffer (D-mannitol 4.098%, Sucrose 2.56%, K_2HPO_4 0.034%, pH 7.3-7.4) and 200 μl of 1% digitonin. After 5 min incubation on ice, the mixture was centrifuged at 8000 RPM for 10 min. The mitochondrial pellet was resuspended in 100 μl of mitochondrial buffer and then used for further experiments.

Brain mitochondrial swelling and Calcium uptake/release inhibition assays

Appropriate amounts of mitochondria were re-suspended in 1 ml swelling assay buffer (150 mM KCl, 2 mM KH_2PO_4, 10 mM HEPES, pH 7.4) and energized with the addition of 1 mM Glutamate and 1 mM Malate. Calcium (200 μM) was added to the assay buffer to trigger mitochondrial swelling. Mitochondrial permeability transition was determined by measuring the rate of change in absorbance at 540 nm on a spectrophotometer.

Initial solubilization of Aβ peptide and preparation of oligomer Aβ

$A\beta_{1-42}$ peptide (lyophilized powder, 1 mg, American Peptide Company, catalog number 62-0-8Q) was stored in sealed glass vials in desiccated containers at −80°C. Prior to resuspension, the lyophilized peptide was allowed to equilibrate to room temperature for 30 min to avoid condensation. Under a chemical fume hood, lyophilized $A\beta_{1-42}$ was resuspended in 100% 1,1,1,3,3,3-hexafluoro-2-propanol (HFIP, Sigma-Aldrich, catalog number 105228) in a polypropylene vial using a glass GasTight® Hamilton syringe with a Teflon plunger. After vortexing, the solution was divided between 3 polypropylene vials and vortexed again. The HFIP was allowed to evaporate in the fume hood for 1 hour, and the resultant clear peptide film was dried under vacuum (6.7 mTorr) in a SpeedVac centrifuge for 10 minutes at 800 × g. The resulting pellet was stored desiccated at -20°C. Directly before use, the aliquots were resuspended in 5 mM anhydrous dimethyl sulfoxide (DMSO, Sigma-Aldrich, catalog number D-2650) by pipette mixing followed by bath sonication for 10 minutes.

Preparation of $A\beta_{1-42}$ Oligomer [43]

$A\beta_{1-42}$ oligomers were prepared by diluting 5 mM of $A\beta_{1-42}$ aliquot in PBS, immediately vortexing for 30 seconds, and incubated at 4°C for 24 hours. Prior to the experiment, the aliquot was diluted in ice-cold culture media to the required concentration. We have successfully prepared oligomer $A\beta_{1-42}$ in our published studies [7; 15; 17; 44; 45]

Measurement of mitochondrial cytochrome c oxidase (CcO) activity

CcO activity was measured as described [3; 7] with a cytochrome c oxidase kit (Sigma). In brief, human neuroblastoma (SK-N-SH) cells were incubated with ABAD inhibitor and Aβ oligomer. After 48 hours incubation, cells were washed twice with PBS, followed by harvesting of cell lysates. The protein concentration was determined by Bradford method. Next, an appropriate volume of cells and enzyme solution was added to 475 μl of assay buffer. The reaction was triggered by the addition of 25 μl freshly prepared ferrocytochrome c substrate solution. Changes of OD550 nm were recorded immediately with an Amersham Biosciences Ultrospec 3100 pro spectrophotometer programmed for 5 s delay, 10 s intervals for a total of six readings.

Measurement of Adenosine-5′-triphosphate (ATP) level

ATP levels were determined using an ATP Bioluminesence Assay Kit (Roche) as our previously described [7; 19]. Briefly, SK-N-SH cells were incubated with ABAD inhibitor and oligomer $A\beta_{1-42}$ at 37°C for 48 hours. Cells were harvested using ATP lysis buffer followed by incubation for 30 minutes on ice. The mixture was centrifuged at 12,000 × g for 10 minutes at 4°C, and the supernatant was collected for the assay. The content of ATP was measured according to the manufacturer's instructions [3; 7]. Light emitted from the luciferase-mediated reaction was captured in a luminescence plate reader (Molecular Devices) at 37°C with an integration time of 10 seconds and calculated from a log-log plot of the standard curve of known ATP concentrations.

Cell survival and toxicity assay

The MTT (3-(4,5-dimethylthiazol-2-yl)-2,5-diphenyltetrazolium_bromide) assay, which is widely used to measure cell proliferation and to screen for anticancer drugs, is used for assessing cell viability. Cells were treated with a range of ABAD compounds (4a & 4b at 1, 10, 50, and 100 μM) for 48 hours and then subjected to MTT reduction assay following the manufacture's instruction.

The trypan blue dye exclusion is commonly used for measuring cell viability and toxicity. 48-66 hours after treatment of ABAD compounds, the trypan blue exclusion experiments were performed. In brief, cells plated in 96-well plates were washed with the balanced salt solution (Hanks-Balanced Salts/HBSS) once, then replaced with HBSS including trypan blue solution to the final concentration of 0.2% (Sigma-Aldrich, St. Louis, MO), and mixed thoroughly. After stand at room temperature for 5 min, cells were washed HBSS again and then maintained in the well with HBSS. Both the stained and unstained cells in each well were counted under a microscope (Nikon E400). The calculated percentage of unstained cells represented the percentage of viable cells. Cell viability (%) = total viable cells (unstained)/ total cells (stained and unstained) ×100.

Statistical analysis

We performed statistical analyses with one-way analysis of variance (ANOVA) using the Statview statistics software (SAS Institute, Version 5.0.1) with Bonferroni/Dumn posthoc test. $P<0.05$ was considered significant. All data are expressed as means ± s.e.m.

Results

ABAD synthetic inhibitors bind to ABAD protein

We selectively synthesized two ABAD inhibitors based on our studies, which showed high affinity of binding to human ABAD along with the improvement of mitochondrial function (Fig. 1). We first evaluated the ABAD inhibitory activity of these synthetic compounds by using *in vitro* SPR to determine whether synthetic compounds bind to human recombinant ABAD protein. The Biacore sensor grams for the binding of compounds 4a and 4b to the immobilized ABAD are shown in Figure 2. The 1:1 Langmuir binding fit model was used to determine the equilibrium dissociation constant (*K*D), and the association (*k*on) and dissociation (*k*off) rate constants by using Equations (1) and (2).

$$dR/dt = k\text{on} \times C \times (R\max - R) - k\text{off} \times R \quad (1)$$

where *R* represents the response unit, *C* is the concentration of the analyte, and

$$K\text{D} = k\text{off}/k\text{on} \quad (2)$$

These results were then evaluated by chi-square analysis. All kinetic parameters are listed in Table 1.

SPR results showed that both compounds 4a and 4b exhibited strong binding affinities for ABAD (Figure 2) with KD values of 496 nM and 291 nM, respectively (Table 1). Compound 4b exhibited slightly higher binding affinity with ABAD than 4a. This was further verified by the ABAD enzymatic activity inhibition assay. These data indicate that ABAD-4a and 4b compounds specifically target to ABAD with the highest affinity binding properties of the synthesized compounds.

Effect on ABAD enzyme activity

To assess the effect of ABAD inhibitors on its enzymatic activity, we determined the ability of the compounds to inhibition SAAC reduction by ABAD (Table 1 and Figure 3). ABAD can catalyze a broad repertoire of substrates, including steroid hormones, fatty acids and alcohols. Here, we utilized NADH-dependent SAAC reduction catalyzed by ABAD to evaluate the inhibitors. By incubating varying concentrations of inhibitors with ABAD, we determined the inhibitory effect on SAAC reduction. Compound 4b exhibited the most potent inhibitory effect on SAAC reduction with IC_{50} at 52.7 μM and Ki at 14.9 μM. Compound 4a showed modest inhibitory effect on SAAC reduction with IC_{50} at 341.9 μM and Ki at 96.6 μM, whereas the previously reported human ABAD inhibitor (AG18051) showed good inhibitory effect with IC_{50} at 92 nM when compared to compounds 4a and 4b. Because enzymatic activity of ABAD is essential for potentiation of Aβ cytotoxicity, it is possible that blocking Aβ–ABAD interaction with small-molecule inhibitors will, in turn, decrease Aβ induced cytotoxicity. The effective concentration of ABAD compound 4a (1 μM) without toxicity is almost 100-fold lower than IC50 (96.6 μM) for inhibition of ABAD activity, suggesting that compound 4a at 1μM would likely be therapeutic effects in AD.

Effect of ABAD inhibitors on mitochondrial function

Mitochondrial swelling in response to Ca^{2+}—As ABAD plays a role in mitochondrial dysfunction and since such dysfunction is relevant to Aβ accumulation and oxidative stress in AD, we first evaluated the effect of the compounds 4a and 4b on mitochondrial permeability transition pore (mPTP) formation. Cortical mitochondria were isolated from mice and subjected to a swelling assay in response to calcium as previously described [7; 18]. Mitochondria responded well to calcium-induced swelling compared to vehicle-treated mitochondria. Addition of 4a or 4b significantly protected mitochondria from calcium-induced swelling in a dose-dependent manner (Figure 4). Compound 4b was a more potent inhibitor of calcium-induced mitochondrial swelling than 4a. The inhibitors did not affect mitochondrial swelling without calcium, suggesting that the inhibitors have no effect on mitochondrial physiology function (Figure 4).

CcO activity—To assess the effect of the inhibitors on Aβ-induced mitochondrial respiratory function, we determined the activity of CcO, which is a key enzyme associated with the mitochondrial respiratory chain. SK-N-SH cells were treated with 5 μM of oligomer Aβ 1-42 in the presence of 1 μM inhibitor (4a or 4b, respectively**)** for 48 hours; samples were then tested for CcO activity. Aβ treatment significantly decreased CcO activity, whereas, addition of ABAD 4a- or 4b compounds rescued CcO activity in Aβ-treated cells compared to vehicle-treated cells (Figure 5A-B). Inhibitor (4a or 4b) alone was without effect on CcO activity in the absence of Aβ (Figure 5).

Levels of ATP—To determine the effect of the ABAD inhibitors on Aβ-induced impairment in energy metabolism, we measured ATP levels. SK-N-SH cells were exposed to 5 μM of Aβ1-42 in the presence of 1μM of compound (4a or 4b, respectively). Then, we measured ATP in cell lysates. As shown in Figure 6, Aβ treatment significantly decreased ATP levels, whereas the addition of ABAD inhibitor rescued ATP activity. ATP levels in cells exposed to ABAD inhibitors were comparable to those of vehicle-treated cells without Aβ, suggesting no toxic effect of the inhibitors on mitochondrial energy metabolism. These data suggest that ABAD inhibitors (4a-b) block mitochondrial dysfunction induced by Aβ (Figure 6).

Effect of ABAD inhibitor on cell survival and toxicity—We evaluated the effect of ABAD inhibitors on cell viability and toxicity using MTT reduction assay and trypan blue exclusion, which are widely used to assess cell survival and toxicity and to screen for drugs toxicity. Cells were treated with a range of concentrations of ABAD compound (4a and 4b) at 1, 10, 50, 100 μM for 48 to 66 hours. Compared to vehicle treatment, cells treated with ABAD compound did not reveal decreased MTT reduction (Fig. 7A), and increased percentage of typan blue-positive cells (Fig. 7B), and abnormal morphology (Fig. 7C), These data suggest that treatment of ABAD inhibitors alone do not have significant cytotoxicity.

Discussion

Here, we evaluated the biological activities of two previously synthesized small molecule ABAD inhibitors on ABAD enzymatic activity and the effects on mitochondrial swelling for mPTP formation, Aβ-mediated abnormal mitochondrial respiratory function and bioenergy. Interestingly, the substitution of methoxy at the 6-position in benzothiazole amine seems to play a crucial role in phosphonate derivative bioactivity. Two benzothiazole phosphonates (compounds 4a and 4b) inhibited ABAD enzymatic binding activity, reduced calcium-induced mPTP formation, decreased Aβ-induced mitochondrial dysfunction, and increased CcO and ATP levels. Clearly, the presence of the hydroxyl group on benzene at the 4-position is essential for ABAD activity, which is consistent with the original design of frentizole and benzothiazole urea scaffold as the active structure. Conversion of frentizole into benzothiazole urea [33] or benzothiazole amino phosphonates [40] results in a remarkable increase in ABAD enzymatic activity potency. Furthermore, the substitution of the heterocyclic aldehyde at the amino position resulted in substantial loss of ABAD inhibitory activity (data not shown).

When the 4-hydroxy substituent was constant, methoxy substitution at the 6-position of benzothiazole amine was generally favorable for ABAD activity, conferring micromolar IC_{50} values for enzymatic reaction inhibition. Furthermore, 6-methoxy-substituted benzothiazole amine displayed potent enzymatic activity and a high therapeutic index. The structurally simple 6-methoxy benzothiazole amine seems to be an optimal substitute for ABAD binding, enzymatic, calcium induced swelling, mitochondrial respiratory function, and energy metabolism inhibition comparable to frentizole and benzothiazole urea derivatives. Additionally, modification of the phosphonate moiety benzthiazole ring has a subtle effect on enzymatic potency (compound 4b). In contrast, benzothiazole phosphate

analogues displayed an overall superior ABAD inhibitory effect in terms of the IC_{50} value and therapeutic index. Thus, these studies shed new light on the design and understanding of benzothiazole phosphate based enzyme inhibitors, which will be helpful for the evolution of this scaffold into clinically useful AD drugs.

The results of our mitochondrial swelling assays indicated that the phosphonate derivatives antagonize calcium-mediated mitochondrial swelling. The *in vitro* assays indicated that compounds 4a and 4b inhibit calcium-dependent brain mitochondrial swelling and calcium uptake and release. More importantly, these compounds largely diminished Aβ-induced mitochondrial dysfunction as shown by increased CcO and ATP in addition to suppression of calcium-induced mitochondrial swelling, demonstrating a protective effect of compounds 4a and 4b on mitochondrial function. The ABAD inhibitors alone did not affect normal mitochondrial and neuronal function. Further, no changes in cell morphology, cell survival and viability were found in cells treated with both ABAD compounds in which concentration of ABAD inhibitor was even up to 100 μM, 100 fold higher than effective dose (1μM), suggesting no toxic effects of the inhibitors on normal cellular function.

Since all assays have been carried out at different experimental conditions required, this could be an explanation that the concentration of ABAD inhibitors depends on the experimental condition. For example, we applied cell-free system to determine the direct effect of the compound on ABAD activity under acute condition *in an in vitro* enzymatic activity in which assays have to be completed in 10 min. In mitochondrial swelling assay, mitochondria were isolated from brain tissue and then treated with calcium *in vitro* for 10-30 min under acute condition (25-100 μM ABAD compound), as compared with the assay to determine the effect of Aβ on mitochondrial function in cell culture (48 hours) as shown in Figures 5-6. In the experiments shown in Figures 5 and 6, we examined the effect of compounds on mitochondrial function in cellular culture system. Our results clearly showed the protective effect of compounds at 1μM on Aβ-induced mitochondrial dysfunction. The results generated from 1μM compound are consistent with the data of the surface plasmon resonance (SPR) with binding affinity (∼300-500 nM). Nevertheless, our studies demonstrate that both compounds significantly improve mitochondrial function by increased complex IV activity, a key enzyme associated with mitochondrial respiratory function, and ATP production in Aβ-rich environment. These data provide the evidence for supporting the conclusion on the protective effect of ABAD compound on Aβ-induced mitochondrial injury.

Novelty of the present approach lies in the use of a phosphonate moiety, which can readily penetrate biological membranes such as the blood-brain barrier and enter the target organ [46-48]. Therefore, phosphate esters are commonly used for prodrug development and exclusively used for water insoluble compounds. [46-50] Future plans include examination of the ability of these compounds to cross the blood brain barrier and further evaluation of the effects on mitochondrial and neuronal function, amyloid pathology, and behavior in an AD mouse model. Additionally, we would like to examine whether our ABAD inhibitors are able to reverse Aβ-initiated mitochondrial dysfunction by incubating neuronal cells with Aβ prior to treatment with the 4a and 4b inhibitors.

In summary, we identified benzthiazole phosphonates derivatives as ABAD inhibitors and successfully developed new small molecule compounds that showed specific ligand binding ability for ABAD. Furthermore, these ABAD inhibitors rescued mitochondrial function diminished by calcium and Aβ. With the goal of improving mitochondrial function in AD, these inhibitors hold potential for therapeutic development

Acknowledgments

This study was supported by grant awards (R37AG037319 and R01GM095355) from the National Institute on Aging and National Institute of General Medical Sciences.

References

1. Perier C, Tieu K, Guegan C, Caspersen C, Jackson-Lewis V, Carelli V, et al. Complex I deficiency primes Bax-dependent neuronal apoptosis through mitochondrial oxidative damage. Proc Natl Acad Sci U S A. 2005; 102(52):19126–31. [PubMed: 16365298]
2. Reddy PH, Beal MF. Amyloid beta, mitochondrial dysfunction and synaptic damage: implications for cognitive decline in aging and Alzheimer's disease. Trends in molecular medicine. 2008; 14(2): 45–53. [PubMed: 18218341]
3. Du H, Guo L, Yan S, Sosunov AA, McKhann GM, Yan SS. Early deficits in synaptic mitochondria in an Alzheimer's disease mouse model. Proc Natl Acad Sci U S A. 2010; 107(43):18670–5. [PubMed: 20937894]
4. Lunnon K, Ibrahim Z, Proitsi P, Lourdusamy A, Newhouse S, Sattlecker M, et al. Mitochondrial dysfunction and immune activation are detectable in early Alzheimer's disease blood. Journal of Alzheimer's disease :JAD. 2012; 30(3):685–710.
5. Quiroz-Baez R, Flores-Dominguez D, Arias C. Synaptic aging is associated with mitochondrial dysfunction, reduced antioxidant contents and increased vulnerability to amyloid-beta toxicity. Current Alzheimer research. 2013; 10(3):324–31. [PubMed: 23305068]
6. Perier C, Bove J, Wu DC, Dehay B, Choi DK, Jackson-Lewis V, et al. Two molecular pathways initiate mitochondria-dependent dopaminergic neurodegeneration in experimental Parkinson's disease. Proc Natl Acad Sci U S A. 2007; 104(19):8161–6. [PubMed: 17483459]
7. Du H, Guo L, Fang F, Chen D, Sosunov AA, McKhann GM, et al. Cyclophilin D deficiency attenuates mitochondrial and neuronal perturbation and ameliorates learning and memory in Alzheimer's disease. Nature medicine. 2008; 14(10):1097–105.
8. Manczak M, Anekonda TS, Henson E, Park BS, Quinn J, Reddy PH. Mitochondria are a direct site of A beta accumulation in Alzheimer's disease neurons: implications for free radical generation and oxidative damage in disease progression. Human molecular genetics. 2006; 15(9):1437–49. [PubMed: 16551656]
9. Lustbader JW, Cirilli M, Lin C, Xu HW, Takuma K, Wang N, et al. ABAD directly links Abeta to mitochondrial toxicity in Alzheimer's disease. Science. 2004; 304(5669):448–52. [PubMed: 15087549]
10. Hauptmann S, Scherping I, Drose S, Brandt U, Schulz KL, Jendrach M, et al. Mitochondrial dysfunction: an early event in Alzheimer pathology accumulates with age in AD transgenic mice. Neurobiology of aging. 2009; 30(10):1574–86. [PubMed: 18295378]
11. Yao J, Irwin RW, Zhao L, Nilsen J, Hamilton RT, Brinton RD. Mitochondrial bioenergetic deficit precedes Alzheimer's pathology in female mouse model of Alzheimer's disease. Proc Natl Acad Sci U S A. 2009; 106(34):14670–5. [PubMed: 19667196]
12. Yan SD, Fu J, Soto C, Chen X, Zhu H, Al-Mohanna F, et al. An intracellular protein that binds amyloid-beta peptide and mediates neurotoxicity in Alzheimer's disease. Nature. 1997; 389(6652): 689–95. [PubMed: 9338779]
13. Yao J, Irwin RW, Zhao L, Nilsen J, Hamilton RT, Brinton RD. Mitochondrial bioenergetic deficit precedes Alzheimer's pathology in female mouse model of Alzheimer's disease. Proc Natl Acad Sci U S A. 2009

14. Du H, Yan SS. Mitochondrial permeability transition pore in Alzheimer's disease: cyclophilin D and amyloid beta. Biochim Biophys Acta. 2010; 1802(1):198–204. [PubMed: 19616093]
15. Guo L, Du H, Yan S, Wu X, McKhann GM, Chen JX, et al. Cyclophilin d deficiency rescues axonal mitochondrial transport in Alzheimer's neurons. PloS one. 2013; 8(1):e54914. [PubMed: 23382999]
16. de Cristobal J, Garcia-Garcia L, Delgado M, Pozo MA, Medina M. A longitudinal FDG-PET study of transgenic mice overexpressing GSK-3beta in the brain. Current Alzheimer research. 2013
17. Du H, Guo L, Yan SS. Synaptic Mitochondrial Pathology in Alzheimer's Disease. Antioxid Redox Signal. 2011
18. Du H, Guo L, Zhang WS, Rydzewska M, Yan SD. Cyclophilin D deficiency improves mitochondrial function and learning/memory in aging Alzheimer disease mouse model. Neurobiology of aging. 2011; 32(3):398–406. [PubMed: 19362755]
19. Yao J, Du H, Yan S, Fang F, Wang C, Lue LF, et al. Inhibition of amyloid-beta (Abeta) peptide-binding alcohol dehydrogenase-Abeta interaction reduces Abeta accumulation and improves mitochondrial function in a mouse model of Alzheimer's disease. J Neurosci. 2011; 31(6):2313–20. [PubMed: 21307267]
20. Takuma K, Yao J, Huang J, Xu H, Chen X, Luddy J, et al. ABAD enhances Abeta-induced cell stress via mitochondrial dysfunction. FASEB journal : official publication of the Federation of American Societies for Experimental Biology. 2005; 19(6):597–8. [PubMed: 15665036]
21. Bolea I, Gella A, Monjas L, Perez C, Rodriguez-Franco MI, Marco-Contelles J, et al. Multipotent, Permeable Drug ASS234 Inhibits Abeta Aggregation, Possesses Antioxidant Properties and Protects from Abeta-induced Apoptosis In Vitro. Current Alzheimer research. 2013; 10(8):797–808. [PubMed: 23919774]
22. Sivanesan S, Tan A, Rajadas J. Pathogenesis of Abeta oligomers in synaptic failure. Current Alzheimer research. 2013; 10(3):316–23. [PubMed: 23036017]
23. Rao VK, Carlson EA, Yan SS. Mitochondrial permeability transition pore is a potential drug target for neurodegeneration. Biochimica et biophysica acta. 2013
24. Valasani KR, Chaney MO, Day VW, Shidu Yan S. Acetylcholinesterase inhibitors: structure based design, synthesis, pharmacophore modeling, and virtual screening. J Chem Inf Model. 2013; 53(8):2033–46. [PubMed: 23777291]
25. Stains CI, Mondal K, Ghosh I. Molecules that target beta-amyloid. ChemMedChem. 2007; 2(12): 1674–92. [PubMed: 17952881]
26. Ghosh AK, Venkateswara Rao K, Yadav ND, Anderson DD, Gavande N, Huang X, et al. Structure-Based Design of Highly Selective beta-Secretase Inhibitors: Synthesis, Biological Evaluation, and Protein-Ligand X-ray Crystal Structure. Journal of medicinal chemistry. 2012; 55(21):9195–207. [PubMed: 22954357]
27. Gravenfors Y, Viklund J, Blid J, Ginman T, Karlstrom S, Kihlstrom J, et al. Correction to New Aminoimidazoles as beta-Secretase (BACE-1) Inhibitors Showing Amyloid-beta (Abeta) Lowering in Brain. Journal of medicinal chemistry. 2012
28. Ogura A, Morizane A, Nakajima Y, Miyamoto S, Takahashi J. gamma-Secretase Inhibitors Prevent Overgrowth of Transplanted Neural Progenitors Derived from Human-Induced Pluripotent Stem Cells. Stem cells and development. 2012
29. Parker MF, Barten DM, Bergstrom CP, Bronson JJ, Corsa JA, Dee MF, et al. 2-(N-Benzyl-N-phenylsulfonamido)alkyl amide derivatives as gamma-secretase inhibitors. Bioorganic & medicinal chemistry letters. 2012; 22(22):6828–31. [PubMed: 23046960]
30. Ozudogru SN, Lippa CF. Disease modifying drugs targeting beta-amyloid. American journal of Alzheimer's disease and other dementias. 2012; 27(5):296–300.
31. Panza F, Solfrizzi V, Frisardi V, Imbimbo BP, Capurso C, D'Introno A, et al. Beyond the neurotransmitter-focused approach in treating Alzheimer's disease: drugs targeting beta-amyloid and tau protein. Aging clinical and experimental research. 2009; 21(6):386–406. [PubMed: 20154508]
32. Frisardi V, Solfrizzi V, Imbimbo PB, Capurso C, D'Introno A, Colacicco AM, et al. Towards disease-modifying treatment of Alzheimer's disease: drugs targeting beta-amyloid. Current Alzheimer research. 2010; 7(1):40–55. [PubMed: 19939231]

33. Xie Y, Deng S, Chen Z, Yan S, Landry DW. Identification of small-molecule inhibitors of the Abeta-ABAD interaction. Bioorganic & medicinal chemistry letters. 2006; 16(17):4657–60. [PubMed: 16781151]
34. Kissinger CR, Rejto PA, Pelletier LA, Thomson JA, Showalter RE, Abreo MA, et al. Crystal structure of human ABAD/HSD10 with a bound inhibitor: implications for design of Alzheimer's disease therapeutics. Journal of molecular biology. 2004; 342(3):943–52. [PubMed: 15342248]
35. Oppermann UC, Salim S, Tjernberg LO, Terenius L, Jornvall H. Binding of amyloid beta-peptide to mitochondrial hydroxyacyl-CoA dehydrogenase (ERAB): regulation of an SDR enzyme activity with implications for apoptosis in Alzheimer's disease. FEBS letters. 1999; 451(3):238–42. [PubMed: 10371197]
36. Milton NG, Mayor NP, Rawlinson J. Identification of amyloid-beta binding sites using an antisense peptide approach. Neuroreport. 2001; 12(11):2561–6. [PubMed: 11496149]
37. Cuadrado-Tejedor M, Cabodevilla JF, Zamarbide M, Gomez-Isla T, Franco R, Perez-Mediavilla A. Age-related mitochondrial alterations without neuronal loss in the hippocampus of a transgenic model of Alzheimer's disease. Current Alzheimer research. 2013; 10(4):390–405. [PubMed: 23545067]
38. Yan Y, Liu Y, Sorci M, Belfort G, Lustbader JW, Yan SS, et al. Surface plasmon resonance and nuclear magnetic resonance studies of ABAD-Abeta interaction. Biochemistry. 2007; 46(7):1724–31. [PubMed: 17253767]
39. Yan SD, Stern DM. Mitochondrial dysfunction and Alzheimer's disease: role of amyloid-beta peptide alcohol dehydrogenase (ABAD). International journal of experimental pathology. 2005; 86(3):161–71. [PubMed: 15910550]
40. Valasani KR, Hu G, Chaney MO, Yan SS. Structure-based design and synthesis of benzothiazole phosphonate analogues with inhibitors of human ABAD-Abeta for treatment of Alzheimer's disease. Chemical biology & drug design. 2013; 81(2):238–49. [PubMed: 23039767]
41. Yan SD, Shi Y, Zhu A, Fu J, Zhu H, Zhu Y, et al. Role of ERAB/L-3-hydroxyacyl-coenzyme A dehydrogenase type II activity in Abeta-induced cytotoxicity. The Journal of biological chemistry. 1999; 274(4):2145–56. [PubMed: 9890977]
42. Caspersen C, Wang N, Yao J, Sosunov A, Chen X, Lustbader JW, et al. Mitochondrial Abeta: a potential focal point for neuronal metabolic dysfunction in Alzheimer's disease. The FASEB journal : official publication of the Federation of American Societies for Experimental Biology. 2005; 19(14):2040–1.
43. Stine WB Jr, Dahlgren KN, Krafft GA, LaDu MJ. In vitro characterization of conditions for amyloid-beta peptide oligomerization and fibrillogenesis. The Journal of biological chemistry. 2003; 278(13):11612–22. [PubMed: 12499373]
44. Du H, Guo L, Wu X, Sosunov AA, McKhann GM, Chen JX, et al. Cyclophilin D deficiency rescues Abeta-impaired PKA/CREB signaling and alleviates synaptic degeneration. Biochim Biophys Acta. 2013
45. Origlia N, Bonadonna C, Rosellini A, Leznik E, Arancio O, Yan SS, et al. Microglial receptor for advanced glycation end product-dependent signal pathway drives beta-amyloid-induced synaptic depression and long-term depression impairment in entorhinal cortex. J Neurosci. 2010; 30(34): 11414–25. [PubMed: 20739563]
46. Somogyi G, Nishitani S, Nomi D, Buchwald P, Prokai L, Bodor N. Targeted drug delivery to the brain via phosphonate derivatives - I. Design, synthesis and evaluation of an anionic chemical delivery system for testosterone. Int J Pharm. 1998; 166(1):15–26.
47. Somogyi G, Buchwald P, Nomi D, Prokai L, Bodor N. Targeted drug delivery to the brain via phosphonate derivatives - II. Anionic chemical delivery system for zidovudine (AZT). Int J Pharm. 1998; 166(1):27–35.
48. Levy D, Ashani Y. Synthesis and Invitro Properties of a Powerful Quaternary Methylphosphonate Inhibitor of Acetylcholinesterase - a New Marker in Blood-Brain-Barrier Research. Biochem Pharmacol. 1986; 35(7):1079–85. [PubMed: 3754444]
49. Rao VK, Reddy SS, Krishna BS, Reddy CS, Reddy NP, Reddy TCM, et al. Design, Synthesis and Anti Colon Cancer Activity Evaluation of Phosphorylated Derivatives of Lamivudine (3TC). Lett Drug Des Discov. 2011; 8(1):59–64.

50. Rao VK, Rao AJ, Reddy SS, Raju CN, Rao PV, Ghosh SK. Synthesis, spectral characterization and biological evaluation of phosphorylated derivatives of galanthamine. European journal of medicinal chemistry. 2010; 45(1):203–09. [PubMed: 19853328]

Abbreviations

APP	amyloid precursor protein
mPTP	mitochondrial permeability transition pore
ATP	Adenosine-5′-triphosphate
ABAD	Amyloid binding alcohol dehydrogenase
Aß	amyloid beta
AD	Alzheimer's disease
SPR	Surface plasmon resonance
CcO	cytochrome c oxidase
SAR	Structure–activity relationship
SAAC	S-acetoacetyl-CoA

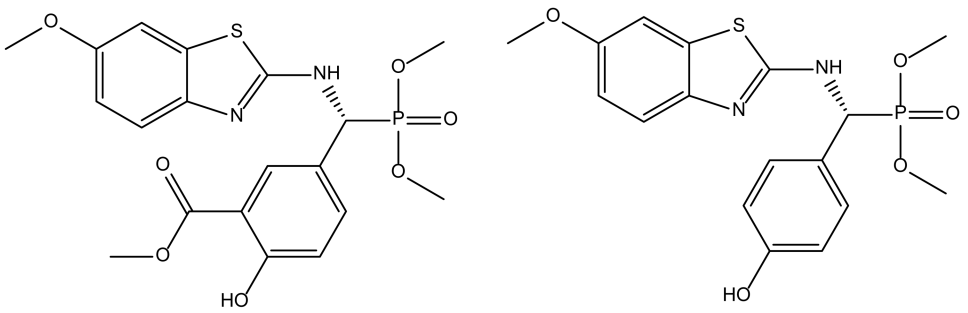

Figure 1.

The structures of the synthesized small molecule ABAD inhibitors 4a and 4b. Hit structures of compounds 4a & 4b obtained by three component one pot reaction of 6-methoxybenzo[d]thiazol-2-amine, aldehydes and dimethyl phosphonate. Compound structures are shown three-dimensional orientation and chiral carbon represents with dashed bonds. Solid lines represent bonds, which are in the plane of the paper and dashed lines to represents bonds that are extend away from the viewer.

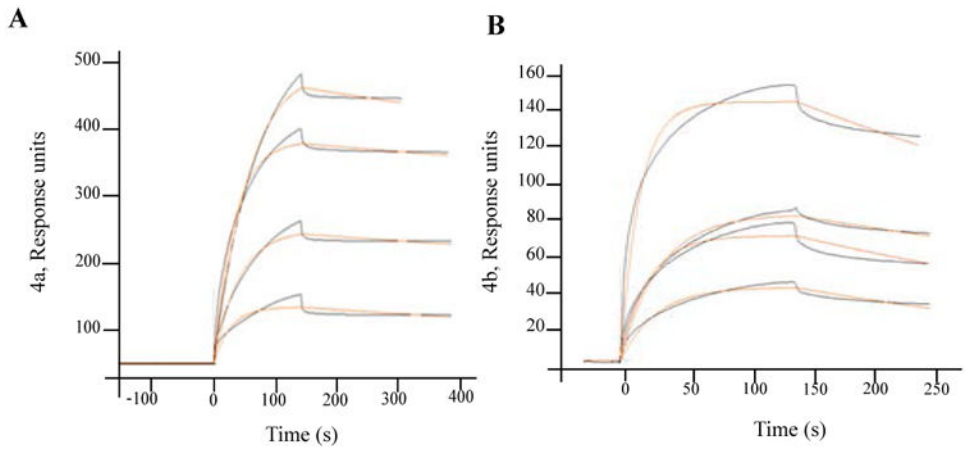

Figure 2.

The synthesized ABAD inhibitors, 4a (A) and 4b (B), bind to immobilized human recombinant ABAD protein in a dose–dependent manner as shown by SPR. Globally fit data (black lines) were overlaid with experimental data (red lines). Human recombinant ABAD protein (10μg/ml) was immobilized directly on the hydrophilic carboxy methylated dextran matrix of the CM5 sensor chip (Biacore) using the standard primary amine coupling reaction according to standard procedures. Compounds (4a, 1, 2, 5, 10 μM & 4b, 1, 5, 10, 15 μM) were injected at flow rate 40 μL/minute for the determination of the kinetic and equilibrium constant. All data analyses were carried out using BIA evaluation software, and sensor grams were processed by automatic correction for nonspecific bulk refractive index effects. The dissociation constant (K_D) was determined as indicated at 25°C

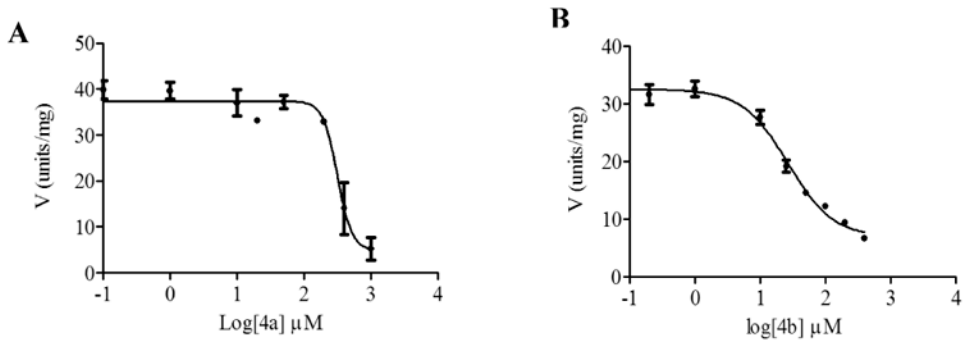

Figure 3.

Inhibition of ABAD enzymatic activity in the presence of benzothiazole phosphonate derivatives (small molecule ABAD inhibitors) 4a (A) and 4b (B). Human ABAD recombinant protein (418 ng/ml) was incubated with or without ABAD compound 4a or 4b (0-200 μM) in 93 mM potassium phosphate buffer (pH 7.3) containing NADH (102 μM). Five minutes after incubation, SAAC were added to the reaction mixture. The reaction was run for a total of 6 min. The decrease of NADH absorbance at 340 nm was determined every 10 seconds. Kinetic data was analyzed by PRISM software to determine IC50 value and Ki. Both compounds (4a and 4b) significantly inhibited ABAD enzymatic activity using SAAC substrate.

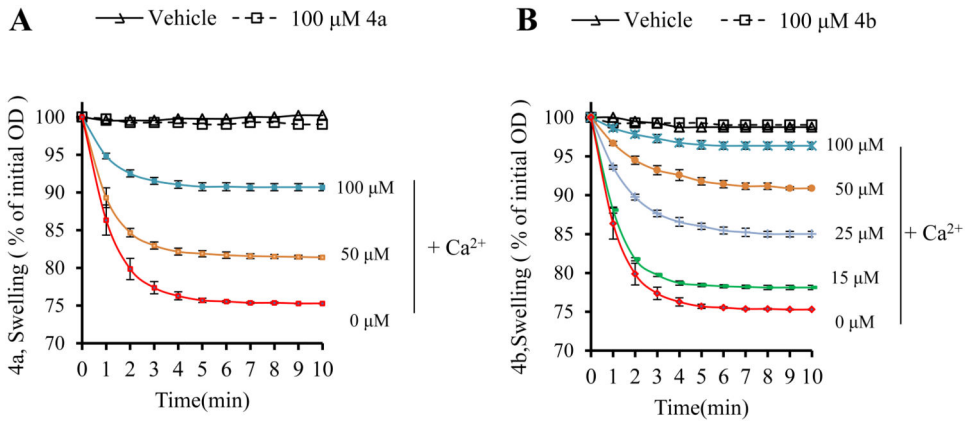

Figure 4.

Effect of Aβ/ABAD inhibitors [4a (A) and 4b(B)] on calcium-induced mitochondrial swelling (red line) compared to vehicle-treated mitochondria (black). The isolated cortical mitochondria (100 μg) were incubated with and without ABAD compound (4a or 4b) on ice for 5 min. Calcium (200 μM) was added to the reaction buffer to trigger mitochondrial swelling. The addition of the indicated concentrations of compounds (0 to 100 μM) attenuated calcium-induced mitochondrial swelling.

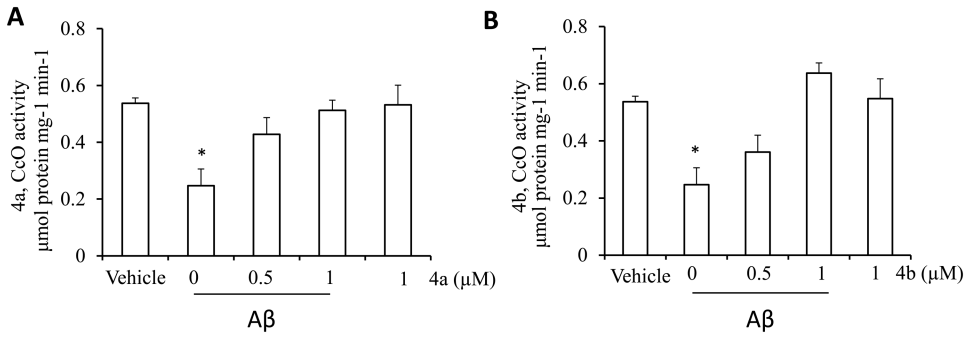

Figure 5.

Effect of ABAD inhibitors (4a (A) and 4b (B)) on Aβ-induced reduction in CcO activity. SK-N-SH cells were treated with 5µM oligomer Aβ plus the indicated inhibitor (4a or 4b) at 0.5 and 1µM, Aβ alone (5 µM), inhibitor alone (1µM), or vehicle without inhibitor, respectively. After 48 hours, CcO activity was measured in cell lysates. *P<0.01 compared to the indicated groups of vehicle, inhibitor (1µM) with Aβ, and inhibitor alone.

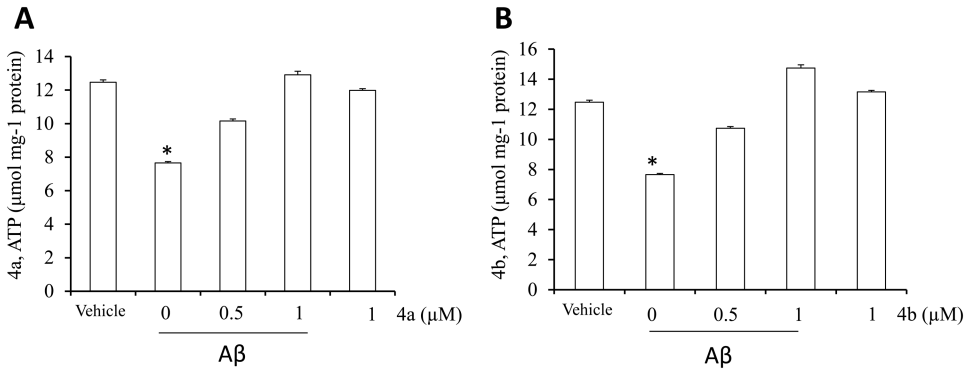

Figure 6.

Effect of ABAD inhibitors [4a (A) and 4b (B)] on Aβ-induced reduction of ATP levels. SK-N-SH cells were exposed to 5μM oligomer Aβ plus the indicated inhibitor (4a or 4b) at 0.5 and 1μM, inhibitor alone (1μM), Aβ alone (5μM), or vehicle without inhibitor, respectively. 48 hours later, ATP levels were determined in cell lysates. *P<0.001compared to the indicated groups of vehicle, inhibitor with Aβ, and inhibitor alone.

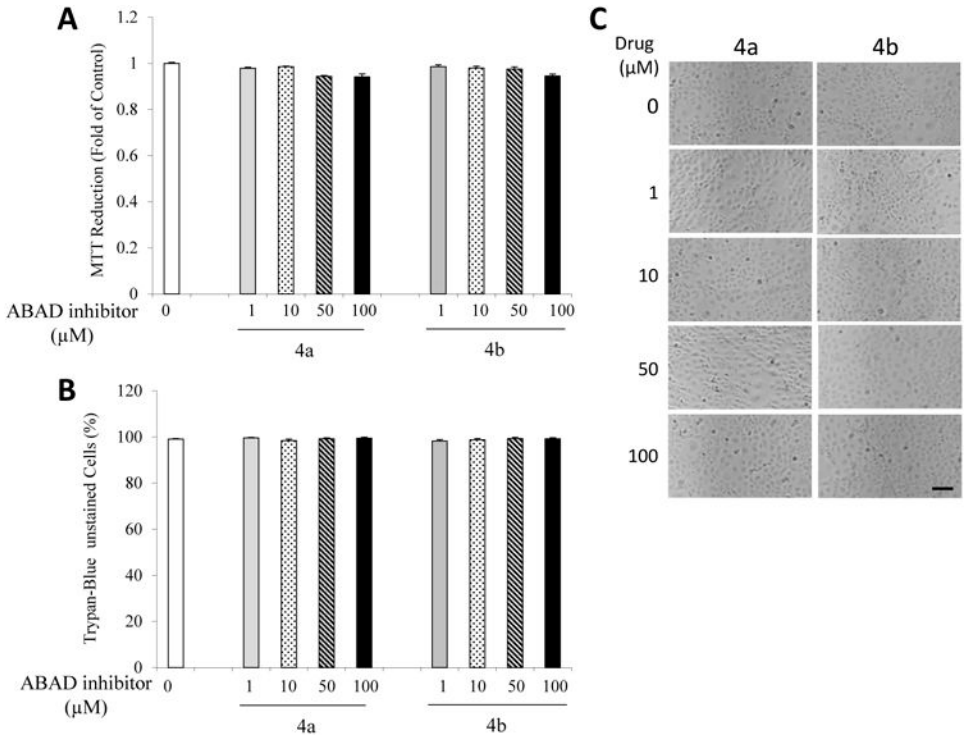

Figure 7.

Effect of ABAD inhibitors on cell survival and toxicity. SK-N-SH human neuronal cell line was incubated with vehicle and ABAD compound (4a or 4b), respectively, at 37°C for 4 -66 hours, and then subjected to the MTT reduction to examine the cell survival (A) and typan blue staining to assess cell death (B). The panel (C) showed the representative morphological images with indicated treatment. The vehicle (0)-treated cells serviced as controls. Scale bar = 50 μm.

Table 1

ABAD enzymatic activity and SPR results.

ABAD Inhibitors	ABAD enzymatic activity IC_{50} (μM)	ABAD enzymatic activity K_i (μM)	SPR KD (nM)
4a	341.89±68.68	96.6±19.4	496
4b	52.7±5.0	14.9±1.4	291